The 2010 Interferometric Imaging Beauty Contest

Fabien Malbet[a†], William Cotton[b], Gilles Duvert[a†], Peter Lawson[c], Andrea Chiavassa[d], John Young[e], Fabien Baron[f], David Buscher[e], Sridharan Rengaswamy[g], Brian Kloppenborg[h], Martin Vannier[i], Laurent Mugnier[j]

[a]Lab. d'Astrophysique de Grenoble (LAOG), UMR 5571 Univ. J. Fourier/CNRS, BP 53, F-38051 Grenoble cedex 9, France;
[b]National Radio Astronomy Obs., 520 Edgemont Road, Charlottesville, VA 22903, USA;
[c]Jet Propulsion Lab., California Institute of Technology, Pasadena, CA 91109, USA;
[d]Max-Planck-Institut für Astrophysik, Karl-Schwarzschild-Str. 1 D-85741 Garching, Germany;
[e]Astrophysics Group, Cavendish Lab., JJ Thomson Avenue, Cambridge CB3 0HE, UK;
[f]Univ. of Michigan, 941 Dennison Building, 500 Church Street, Ann Arbor, MI 48109, USA;
[g]European Southern Obs. Casilla 19001, Santiago 19, Chile;
[h]Univ. of Denver, 2112 East Wesley Ave, Room 211, Denver, CO 80208, USA;
[i]Laboratoire H. Fizeau, Univ. de Nice-Sophia Antipolis, parc Valrose, F-06108 Nice, France;
[j]ONERA/DOTA, BP 72, F-92322 Châtillon cedex, France;
[†]Jean-Marie Mariotti Center (JMMC), France;

ABSTRACT

We present the results of the fourth Optical/IR Interferometry Imaging Beauty Contest. The contest consists of blind imaging of test data sets derived from model sources and distributed in the OI-FITS format. The test data consists of spectral data sets on an object "observed" in the infrared with spectral resolution. There were 4 different algorithms competing this time: BSMEM the Bispectrum Maximum Entropy Method by Young, Baron & Buscher; RPR the Recursive Phase Reconstruction by Rengaswamy; SQUEEZE a Markov Chain Monte Carlo algorithm by Baron, Monnier & Kloppenborg; and, WISARD the Weak-phase Interferometric Sample Alternating Reconstruction Device by Vannier & Mugnier. The contest model image, the data delivered to the contestants and the rules are described as well as the results of the image reconstruction obtained by each method. These results are discussed as well as the strengths and limitations of each algorithm.

Keywords: Astronomical software, closure phase, aperture synthesis, imaging, optical, infrared, interferometry

1. INTRODUCTION

This paper presents the results of the fourth Optical/IR Interferometry Imaging Beauty Contest following similar contests in 2004,[1] 2006[2] and 2008.[3] These contests are intended to encourage the development and distribution of techniques and software for imaging optical/IR astronomical interferometric data. Due to the phase noise introduced by atmospheric turbulence, phase information measured on individual interferometric baselines is strongly corrupted. However, the "closure phase" or "bi-spectrum" technique uses the sums of measured phases around closed loops of baselines in which all phase contributions other than those due to the target enter twice but with opposite sign and therefore cancel. This technique has been used to image data from COAST, NPOI, IOTA, ISI, CHARA and the VLTI/AMBER interferometers.

The contest consists of imaging data sets of targets whose details are unknown to the contest participants but are derived from models whose Fourier transforms are sampled in the pattern of a typical interferometer. The contest data is then the visibility square and closure phases derived from this data set as would be measured

Send correspondence to F. Malbet
E-mail: Fabien.Malbetobs.ujf-grenoble.fr

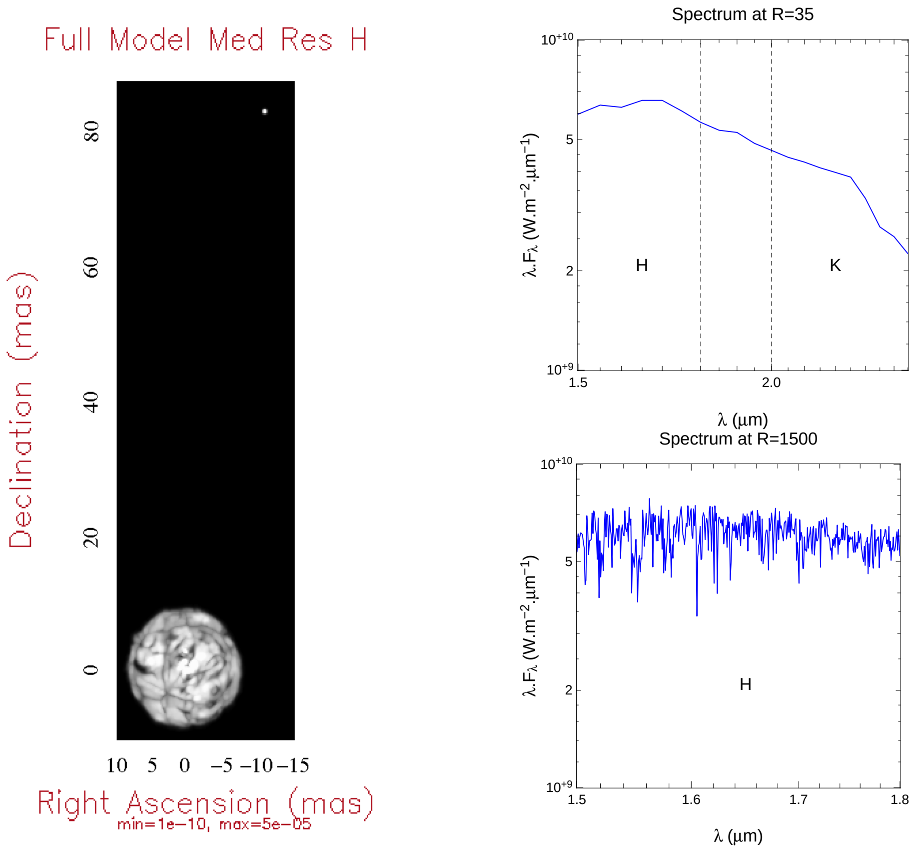

Figure 1. Left: Original image of the first plane of the data cube used to produce the 2010 Beauty Contest. It consists in a stellar surface of a supergiant (as in Chiavassa et al. 2009[4]), set at the angular dimension and location of the supergiant γ Cru, and a faint companion located 80 mas to the North-West averaged over the MRH data cube. Right: the spectrum of the supergiant in low resolution (top) and in medium spectral resolution (bottom).

by such an array. In each contest, the targets have become more challenging. In the 2010 contest, the team who has generated the data set has mimicked AMBER/VLTI data allowing spectral imaging with the delivery of spectrally-dispersed Fourier data cubes. The object is a supergiant with a faint companion. This contest is being conducted by the Working Group on Image Reconstruction of IAU Commission 54.

2. CONTEST MODEL, DATA AND GUIDELINES

The 2010 challenge consisted in reconstructing the surface features of a supergiant hosting a much fainter and unresolved companion located at 8 stellar radii.

2.1 The original data

The original image comes from the work of Chiavassa et al. (2009)[4] who computed intensity maps at different wavelengths (corresponding to broadband filters H and K) with the radiative transfer code OPTIM3D from snapshots of the 3D hydrodynamical simulation (code CO^{5}BOLD) of a red supergiant star. They used in this work a model with stellar parameters close to those of Betelgeuse:[5] a 12 $M_\odot$ stellar mass, a luminosity averaged over spherical shells and time of L=93000±1300 $L_\odot$, an effective temperature of $T_{\rm eff}$=3490±13 K, a radius of R=832±0.7 $R_\odot$, and surface gravity log(g)=-0.337±0.001. The numerical resolution is 235^3 with a grid spacing of 8.6 $R_\odot$. The model of this M0 40 mas supergiant has been scaled to a ≈20 mas star and set at the location of γ Cru whose angular size matches and could arguably have such features, and is conveniently imageable by the VLTI.

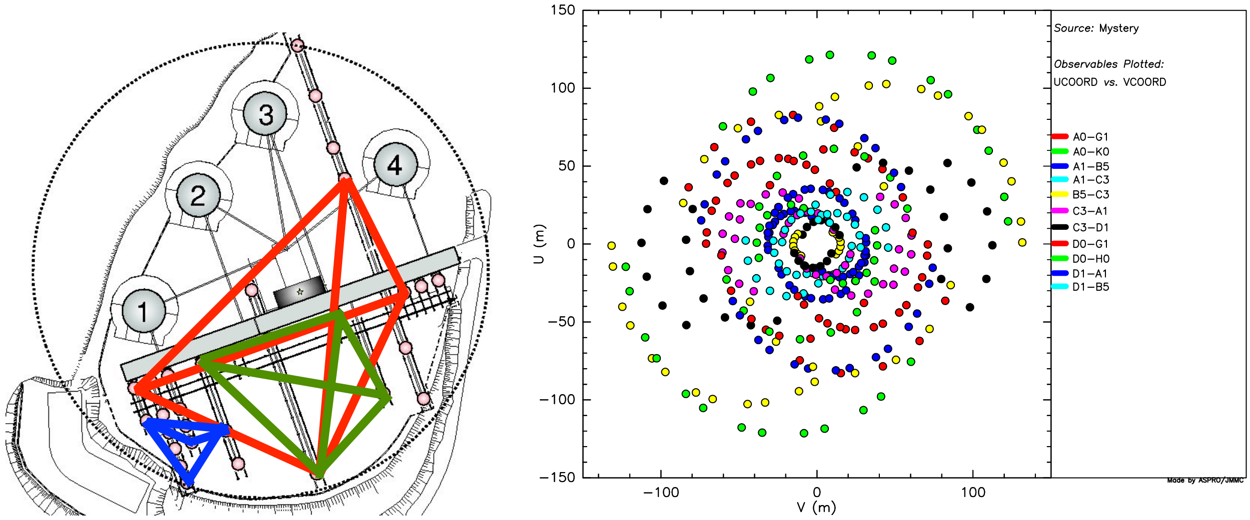

Figure 2. Baseline configuration at VLTI (left) used for the contest and the resulting (u, v) plane coverage (right).

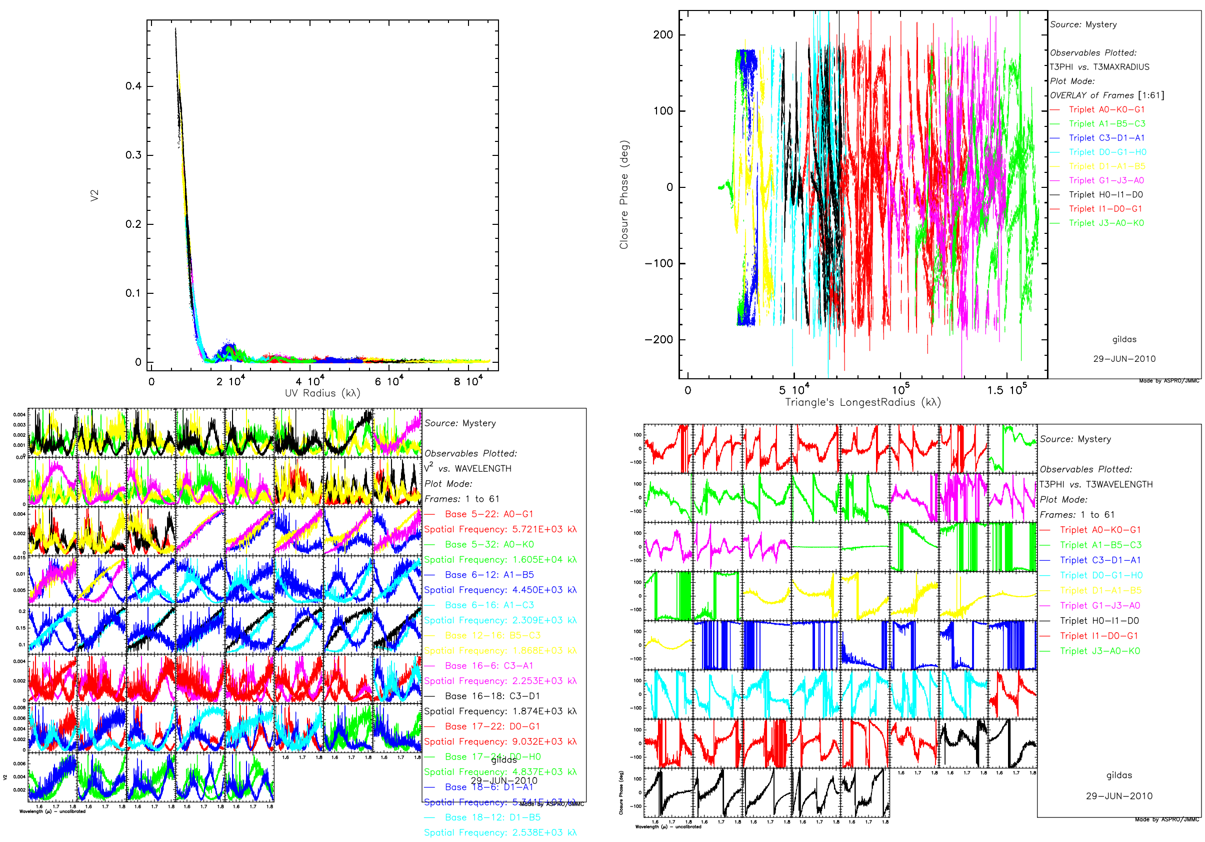

Figure 3. Interferometric data delivered to the contestants. Left: squared visibilities; right: closure phases. Top: wrt. the spatial frequencies; bottom: wrt. the wavelength.

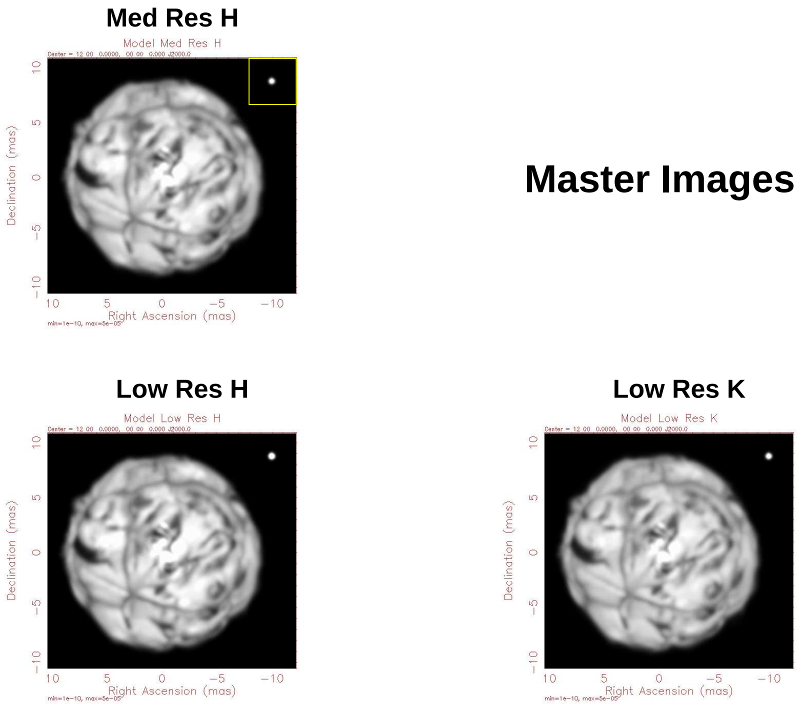

Figure 4. Gray master images used for the comparison. The upper left is the gray image resulting from the medium resolution data cube in H band, the left lower image from the low resolution in H band and the right lower image to the low resolution in K band. In the upper right of each image the inset represents the part of the image where the unresolved companion is located. It has been moved closer to the stellar surface in order to have better details of both components.

To add a bit of spice, we also put a faint companion at distance $\rho = 84.28\,\mathrm{mas}$ at $PA = 261.31\,\mathrm{degrees}$. This separation is only 8 stellar radii of the stellar source, hence resolving the companion is well beyond the capabilities of adaptive optics instruments like NACO. The companion is 5 magnitudes fainter than the star. This translates to an A0V-like star or so in terms of stellar type. It should be visible in the image reconstruction at least the medium resolution H images, because of the small ripple it gives at very low V2. Also, it would be interesting to see if phase closure 'nulling' signatures like those described in Chelli et al. 2009[6] permit to retrieve the companion spectrum.

Figure 1 displays the original image with the stellar surface in the South East corner and the unresolved companion in the North-West region.

2.2 Interferometric data

The simulations used here have been made with the `ASPRO` package.[7] `ASPRO` simulates the observation by an interferometer of a science astronomical object, at one or several times and delivers simulated interferometric observables in the OIFITS format.[8] The interferometric chain is modeled as the combination of an interferometer infrastructure and focal instruments. The interferometer infrastructure comprises the telescopes, delay lines, tip-tilt correctors, adaptive optics, and fringe trackers. It adds geometrical requirements such as the positions and sizes of the telescopes apertures at the time of observation with respect to the position of the science object and the geometrical delays thus induced between each pair of telescopes. In addition, it includes environmental constraints such as the atmospheric seeing, the different horizons seen by telescopes and technical limitations (limits on the delay-line strokes, flux dependence of active optical elements...).

Two observations of the synthesized γ Cru object were simulated: a H-band medium spectral resolution (MRH) at $R = 1500$, and a simultaneous H- and K-band low spectral resolution (LRHK) at $R = 35$ with the 1.8-m telescopes of VLTI, which are meant for imaging. The (u, v) coverage for imaging has been simulated for the 3T instrument AMBER, using series of triplets taken in the quadruplets proposed by ESO/VLTI for their

period 87: A0-G1-K0-J3, A1-B5-C3-D1, D0-G1-H0-I1. This configuration can be achieved in 3 days, one day per quadruplet by switching AMBER beams every 30 minutes between 3 triplets of the quadruplets: A0-G1-K0, A0-J3-K0, A0-G1-J3 A1-B5-C3, A1-C3-D1, A1-B5-D1 D0-G1-H0, D0-H0-I1, DO-G1-I1.

The basic idea was to test the reconstruction methods for spectrally-dispersed data. To enable a channel-per-channel reconstruction, the signal-to-noise ratio per spectral channel needed to be good, thus the object bright. The size of the star and the principal features could be retrieved with a 'grey' image reconstruction, or by binning a number of spectral channels. It could be possible also to use the 'grey' or 'binned' images as a starter for a finer, channel by channel, reconstruction or by forcing the reconstruction support inside a 20 mas stellar disc.

2.3 Contest rules

This year, there was two sets of judgings:

1. one for "gray" images (it was agreed that "gray" meant uniform weighting of spectral channels) derived from the provided datasets assuming a constant target structure with wavelength:
   (a) one derived from all the channels in the `Mystery-Med_H.oifits.gz` data set,
   (b) one from the first 10 (short wavelengths) channels of the `Mystery-Low_HK.oifits.gz` data set and
   (c) the third from the second 10 channels of the `Mystery-Low_HK.oifits.gz` data;

   and
2. a second for a "spectral" image allowing channel to channel differences.

Submissions could be sent for either or both categories. Spectral image submissions could be either as a single three dimensional FITS cube with 512 planes or as 512 separate single plane FITS images.

3. CONTEST SUBMISSION

3.1 BSMEM

by Young, Baron and Buscher (University of Cambridge)

The BSMEM (BiSpectrum Maximum Entropy Method) software was first written in 1992 to demonstrate image reconstruction from optical aperture synthesis data, and has been extensively enhanced and tested since then. It applies a fully Bayesian approach to the inverse problem of finding the most probable image given the evidence, making use of the Maximum Entropy approach to maximize the posterior probability of an image. BSMEM is available free-of-charge to the scientific community on submission of the academic licence agreement at `http://www.mrao.cam.ac.uk/research/OAS/bsmem.html`.

BSMEM uses a trust region method with non-linear conjugate gradient steps to minimise the sum of the log(likelihood) (chi-squared) of the data given the image and a regularization term expressed as the Gull-Skilling entropy $\sum_k (I_k - M_k - I_k \log(I_k/M_k))$. The model image M_k is usually chosen to be a Gaussian, a uniform disk, or a delta-function centered in the field of view, which conveniently fixes the location of the reconstructed object (the bispectra and power spectra being invariant to translation). This type of starting model also acts as a support constraint by penalising the presence of flux far from the centre of the image. An important advantage of BSMEM is the automatic Bayesian estimation of the hyperparameter alpha that controls the weighting of the entropic prior relative to the likelihood. BSMEM can also perform a Bayesian estimation of missing triple amplitudes and their associated errors from the powerspectra data - it was necessary to use this capability for the contest data.

We found that BSMEM was very slow (runtimes upwards of 24 hours on a standard PC) to converge to a well-fitting (reduced chi-squared < 5) solution when given data from multiple spectral channels and an uninformative prior - probably in large part due to the wavelength-dependence of the object. Thus we followed the approach of finding an image whose low spatial frequencies were compatible with the data, and reconstructing each spectral

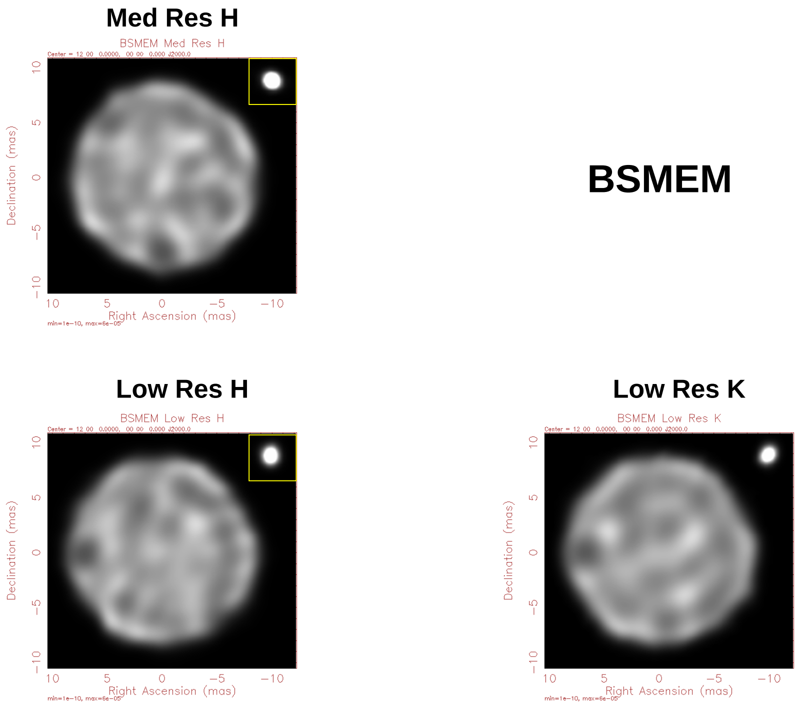

Figure 5. Gray scale images of BSMEM images as used in the comparison. Display is the same as in Figure 4.

channel separately using this as the model image. The reconstructed images from each spectral channel were then averaged to generate the three gray images specified by the contest organizers.

In particular, we found that BSMEM did eventually converge using low-spatial-frequency data (baselines up to 60m) from the first 8 spectral channels of the low-spectral-resolution dataset. The resulting image was convolved with a Gaussian with FWHM equal to the finest fringe spacing and thresholded to remove features judged to be noise. This convolved image was used as the model image for the subsequent reconstructions of individual spectral channels, which typically converged after 70 to 250 iterations (of order 30 minutes on a standard PC). To generate the gray submissions, the spectral channels were averaged with uniform weighting, and pixels below a specified threshold in the average image were set to zero. The threshold value was chosen to remove most of the obvious circumstellar artefacts, each of which typically appeared in the one spectral channel only.

In the submitted FITS images, North is up and East is to the left when the standard display convention for FITS images is followed. I also attach a reconstruction (0.5 mas/pix) of the contest binary to confirm this. BSMEM does not impose any resolution on the reconstructed image, except for the pixel size which was chosen to be 0.4 mas for the mystery object (6 pixels per fastest fringe). The size of the smallest believable features in the reconstructions is 0.8 mas, so you may wish to use this resolution for comparison with the truth images.

We are confident the following features are real:

- The "stellar" disk and its limb-darkening
- The compact companion close to the north edge of the maps
- The more prominent stellar surface structures (in particular, the central bright spot and the two prominent bright spots in the northern hemisphere, the dark area close to the southern disk edge, and probably the dark area close to the eastern disk edge)
- The changes in the contrast of the stellar surface structures with wavelength

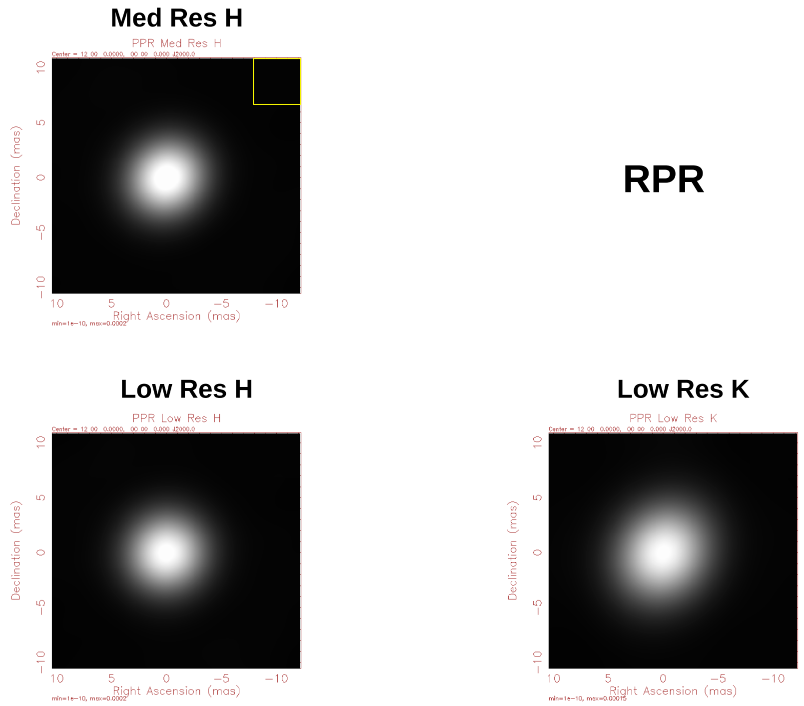

Figure 6. Gray scale images of RPR images as used in the comparison. Display is the same as in Figure 4.

3.2 RPR

by Rengaswamy (European Southern Observatory)

For the contest data, images of size 512×512 pixels were synthesized over a field-of-view of 0.2048×0.2048 arcsec, in each of the spectral channels (10 each in LRH and LRK and, 512 in MRH). For contest #1, the individual images were averaged over the spectral line channels to obtain 3 2-D images. For contest #2, the individual images are stored in 10 data cubes.

I think, the mystery object is a binary; at least it is the most obvious feature; there could be some extended background features but they are not reconstructed clearly. There is a central bright object, which is well resolved disk, with angular size of about 14 mas. The secondary is at a distance of 17.3 ± 0.56 arcsec, with position angle of 153 deg (east of north). The secondary is fainter by a factor of 40. There could be some extended background in both the images, but they are not reconstructed.

Procedure (software)

1. Visibility amplitude was obtained directly from V^2 data.
2. Bispectra were estimated for a "model" source. Then observed bispectra were substituted in place of the model bispectra and a phase map was obtained using a recursive reconstruction method.
3. Complex visibilities (obtained from step 1 and 2) were weighted according to their signal-to-noise ratio, averaged at grid points as and when required, weighted by a tapering function (Hanning function) and then Fourier inverted.
4. The map is then CLEANED over the central region and the CLEAN residuals are added.

Known issues

Perhaps due the basic assumptions of "CLEAN", the background is not reconstructed. The individual reconstruction in spectral channels show some 180 degrees ambiguity for the secondary- this could be possibly because of incorrect phase information.

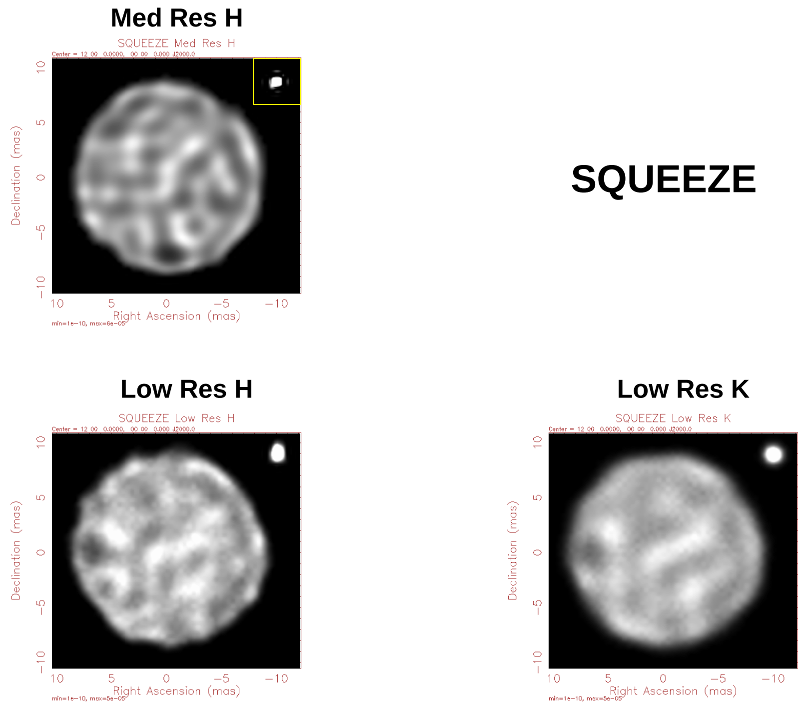

Figure 7. Gray scale images of SQUEEZE images as used in the comparison. Display is the same as in Figure 4.

Note

The reconstructed images contained several bright points, which, I suspected, are arising from amplitude errors. So I did a "PHASE ONLY RECONSTRUCTION", and found that these bright features (4 of them) go away. Thus, for the results I presented here, I did phase only reconstructed images (to avoid artifacts). I did not use visibility amplitude and differential phases. I used only closure phases.

3.3 SQUEEZE

by Baron, Kloppenborg and Monnier (University of Michigan and University of Denver)

SQUEEZE is a new software developped by Fabien Baron and John Monnier at the University of Michigan, with the collaboration of Brian Kloppenborg from the University of Denver. It is the spiritual sucessor of MACIM, but also benefits from code exchange with the GPAIR project and the model-fitting code Fitness. Both SQUEEZE and GPAIR are in their infancy, and are described for the first time in these proceedings. SQUEEZE uses a Markov Chain Monte Carlo engine, and relies on simulated annealing and parallel tempering to sample the posterior probability distribution of the image and find its global maximum. Contrary to other software, it does not explicitly search for the most probable "mode" image, but collects/averages statistics around it. A secondary gradient-based engine is being added to precisely determine the mode image. Finally a complementary module currently allows simultaneous model-fitting and image reconstruction. Novel capabilities for interferometry such as wavelet regularization within the compressed sensing framework and imaging on spheroids are also being implemented.

For this contest we uses the quantified Shannon entropy for our first trials to obtain a draft image. We then convolved it by a PSF corresponding to a 50-m baseline size to generate a prior image, which we subsequently used within a Poisson entropy. Quantification allowed the full process to be free of hyperparameters.

Our submission consists only of the grey images as we lacked the time to implement an optimal algorithm for wavelength-dependent images (full cube reconstruction with SED and differential visibility code) compatible with our engine. For the low spectral resolution images, convergence ("burn-in") to the lowest chi-squared was achieved for 512×512 in less than a minute, after that the image was created in about 30 minutes on a typical

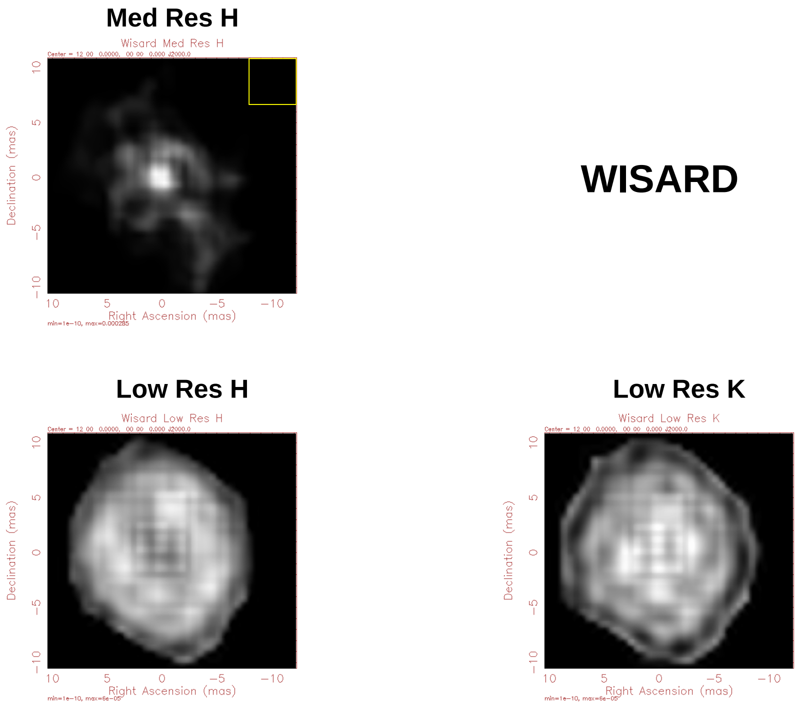

Figure 8. Gray scale images of WISARD images as used in the comparison. Display is the same as in Figure 4.

PC, by averaging 4000 posterior samples. Reconstructing the medium spectral resolution image with this number of samples was a much more computer intensive task, requiring about two hours, but uneventful otherwise.

As an experiment, simultaneous imaging/model-fitting of a bandwidth-smeared uniform disk allowed us to determine the position of the object lying 80 degrees East of North as (-12.5, 84.7) mas, that its flux represents about 2% of the flux of the image, and that it seems to be a point source in H (diameter < 0.4 mas) and barely resolved in K (diameter < 0.8 mas). The 64×64 images of the stellar surface obtained in this "imaging/fitting" mode were obtained in less than 2 minutes, were slightly better than the "full imaging" we finally submitted. However we felt this would depart from the pure imaging spirit of the contest, imaging a point source being for us part of the challenge. Note that forcing a different regularization on the point source location would have been possible but was not attempted.

What we think is real is the limb-darkened stellar surface of the primary, including the main discernable features (dark spot on the East side for the low resolution datafiles and South for the medium one, brighter features in the center, darker South West region). The differences between the H and K images (apart from the visible effects of the lower resolution in K) are subtle but are probably real too. Finally the companion (Jupiter ?) has no discernable features but is obviously real. The point source object is not as optimally represented as we would wish without the model-fitting mode. The lower dynamical range allowed by the engine (flux quantification and propagation of flux quanta) does not easily allow us to represent such a strong point source. Finally, exploring the posterior distribution reveals unlikely features such as slight ejection in H west of the star or an ejection disk 50 mas around the star which we do not believe are part of the truth image and attribute to noise fitting regions.

3.4 WISARD

by Vannier and Mugnier (Université of Nice and ONERA)

WISARD is an image reconstruction method developed by Meimon et al.[9,10] and designed to process optical long baseline interferometry data, namely squared visibilities and closure phases. It draws from self-calibration algorithms in radio-interferometry,[11] but uses a more precise approximation of the data model[12] than first attempts.[13] WISARD relies on an explicit modeling of the missing phase information and allows one to obtain a

Table 1. Comparison between the reconstructed images and the initial images. The best scores are the lowest.

	LR-H	LR-K	MR-H	Combined Gray	*H* Cube
BSMEM	6.6	5.9	10.4	7.6	13.9
SQUEEZE	7.9	5.9	22.7	12.2	[not submitted]
WISARD	11.5	11.4	37.9	20.3	47.0
PPR	40.0	31.8	42.1	38.0	45.6

convex intermediate image reconstruction criterion. The adopted approach consists in jointly finding the object and a phase vector, corresponding to phase components in the null space of the closure operator, that best fit the data.

WISARD also draws from Bayesian inversion methods in the sense that it incorporates prior information on the sought object through a regularization metric. Three regularization metrics are currently implemented: (a) a basic Power Spectral Density-based regularization, often used in single-aperture imaging,[14] which was used in the 2004 IBC;[1, 1] (b) a non-quadratic, spike-preserving regularization,[10] appropriate for objects that mix point-like features and smooth areas; (c) a so-called soft-support regularization, proposed specifically for long baseline interferometry[15] in order to enforce compactness of the sought object and thus interpolate missing frequencies. WISARD is a free (open source) software developed in IDL and has been used to process several astronomical datasets.[16–18]

Concerning the images of the 2010 Beauty Contest, the FOV for the reconstructed K-band image is 89 mas with 161×161 pixels (ie. a pixel size of $0.553 \times 0.553\,\mathrm{mas}^2/\mathrm{pix}$) and whereas the FOV and number of pixels for the H-band reconstructed images (both grey-LR and chromatic-MR) are respectively 107.4 mas and 193 mas, which means almost the same pixel size ($0.557 \times 0.557\,\mathrm{mas}^2/\mathrm{pix}$). No rotation was applied to the images, they are oriented the standard way, North-East.

Concerning which features are interpreted as 'real', We certainly think that the central part is real, with a peak surrounded by a fairly compact (although not very regular) structure, oriented mainly from top-left to bottom-right of the image. We tend to think as well that most of the irregular structures surrounding this central compact part belong to a "ring" or a "layer", of diameter approximately half of the larger field, i.e. about 50 mas. As for the outest, and most irregular structures, they might well be reconstruction artifacts. We have had troubles regularizing such artifacts properly, given the very large computat ion time (lots of visibilities, large field,... and many spectral channels).

4. COMPARISON METRICS AND CONTEST RESULT

To compare the reconstructed images which were submitted and the initial data cube images, we used the following procedure:

1. Align all images using the centroid of a Gaussian fitted to the main star. The image should not be Gaussian but this gives a good alignment.
2. Interpolate submitted images to the grid of the model images.
3. Model images were convolved by a 0.4 mas circular Gaussian to get the resolution a little closer to that of the submissions.
4. Normalize all planes in all images such that the sum of the pixels in the box defined by corners [25,25] and [214,214] was 1.0. This includes the model images.
5. The comparison value for each image is 10^6 times the RMS pixel-to-pixel difference between the submission and the model in the region defined by corners [25,25] and [214,214] plus the region defined by the corners [246,1013] and [266,1034] for each plane. These cover the regions of the primary star and the companion. For the gray comparison, the final value is the average of those for the three images. For the cube, the final value is the average over all planes.

Figure 9. The 2010 Interferometry Imaging Beauty Contest jury presenting the award for the winning entry to the representative of the BSMEM team. From left to right: P. Lawson, F. Baron, F. Malbet, G. Duvert.

The best scores are the lowest. They are reported in Table 1. The first two contests have been won by the BSMEM entry and the last one by MIRA. While the top two contestants have very similar results, the BSMEM entry represented by F. Baron has achieved the lowest score and is thereby declared the winner of this year's contest (see Fig. 9).

5. CONCLUSION

Some of the participating algorithms were able to perform relatively faithful image reconstruction on the combination of a resolved stellar surface and an unresolved faint companion. The new type of data set consisting in spectral cubes was a challenge for all the contestants, mostly because the computation time became an important issue. There was no global image reconstruction, just one spectral channel by one spectral channel reconstruction and no use of differential quantities. There were no attempts to get a spectrum of the companion relative to the star so far. The organizer also hope that this type of exercize will allow the different teams to test their the algorithms in order to accomodate the full information contained in spectral data and improve their faithfulness.

ACKNOWLEDGMENTS

Work by PRL was undertaken at the Jet Propulsion Laboratory, California Institute of Technology, under contract with the National Aeronautics and Space Administration Work by WDC was supported by the National Radio Astronomy Observatory, a facility of the National Science Foundation operated under cooperative agreement by Associated Universities, Inc.

REFERENCES

[1] Lawson, P. R., Cotton, W. D., Hummel, C. A., Monnier, J. D., Zhao, M., Young, J. S., Thorsteinsson, H., Meimon, S. C., Mugnier, L. M., Le Besnerais, G., Thiebaut, E. M., and Tuthill, P. G., "An interferometry imaging beauty contest," *Society of Photo-Optical Instrumentation Engineers (SPIE) Conference Series* **5491**, 886 (2004).

[2] Lawson, P. R., Cotton, W. D., Hummel, C. A., Baron, F., Young, J. S., Kraus, S., Hofmann, K., Weigelt, G. P., Ireland, M., Monnier, J. D., Thiébaut, E., Rengaswamy, S., and Chesneau, O., "2006 interferometry imaging beauty contest," *Society of Photo-Optical Instrumentation Engineers (SPIE) Conference Series* **6268** (2006).

[3] Cotton, W., Monnier, J., Baron, F., Hofmann, K., Kraus, S., Weigelt, G., Rengaswamy, S., Thiébaut, E., Lawson, P., Jaffe, W., Hummel, C., Pauls, T., Schmitt, H., Tuthill, P., and Young, J., "2008 imaging beauty contest," *Society of Photo-Optical Instrumentation Engineers (SPIE) Conference Series* **7013** (2008).

[4] Chiavassa, A., Plez, B., Josselin, E., and Freytag, B., "Radiative hydrodynamics simulations of red supergiant stars. I. interpretation of interferometric observations," *A&A* **506**, 1351–1365 (2009).

[5] Levesque, E. M., Massey, P., Olsen, K. A. G., Plez, B., Josselin, E., Maeder, A., and Meynet, G., "The Effective Temperature Scale of Galactic Red Supergiants: Cool, but Not As Cool As We Thought," *ApJ* **628**, 973–985 (2005).

[6] Chelli, A., Duvert, G., Malbet, F., and Kern, P., "Phase closure nulling. Application to the spectroscopy of faint companions," *A&A* **498**, 321–327 (2009).

[7] Duvert, G., Bério, P., and Malbet, F., "ASPRO, a software to prepare observations with optical interferometers," *SPIE* **4844**, 295 (2002).

[8] Pauls, T. A., Young, J. S., Cotton, W. D., and Monnier, J. D., "A Data Exchange Standard for Optical (Visible/IR) Interferometry," *PASP* **117**, 1255–1262 (2005).

[9] Meimon, S. C., Mugnier, L. M., and Le Besnerais, G., "A novel method of reconstruction for weak-phase optical interferometry," *Society of Photo-Optical Instrumentation Engineers (SPIE) Conference Series* **5491**, 909 (2004).

[10] Meimon, S., Mugnier, L. M., and Le Besnerais, G., "Self-calibration approach for optical long-baseline interferometry imaging," *Journal of the Optical Society of America A* **26**, 108 (2008).

[11] Cornwell, T. J. and Wilkinson, P. N., "A new method for making maps with unstable radio interferometers," *MNRAS* **196**, 1067–1086 (1981).

[12] Meimon, S., Mugnier, L. M., and Le Besnerais, G., "Convex approximation to the likelihood criterion for aperture synthesis imaging," *Journal of the Optical Society of America A* **22**, 2348–2356 (2005).

[13] Lannes, A., "Weak-phase imaging in optical interferometry," *Journal of the Optical Society of America A* **15**, 811–824 (1998).

[14] Conan, J., Mugnier, L. M., Fusco, T., Michau, V., and Rousset, G., "Myopic deconvolution of adaptive optics images by use of object and point-spread function power spectra," *Appl. Opt.* **37**, 4614–4622 (1998).

[15] Le Besnerais, G., Lacour, S., Mugnier, L. M., Thiebaut, E., Perrin, G., and Meimon, S., "Advanced Imaging Methods for Long-Baseline Optical Interferometry," *IEEE Journal of Selected Topics in Signal Processing, Vol. 2, Issue 5, p.767-780* **2**, 767–780 (2008).

[16] Lacour, S., Meimon, S., Thiébaut, E., Perrin, G., Verhoelst, T., Pedretti, E., Schuller, P. A., Mugnier, L., Monnier, J., Berger, J. P., Haubois, X., Poncelet, A., Le Besnerais, G., Eriksson, K., Millan-Gabet, R., Ragland, S., Lacasse, M., and Traub, W., "The limb-darkened Arcturus: imaging with the IOTA/IONIC interferometer," *A&A* **485**, 561–570 (2008).

[17] Haubois, X., Perrin, G., Lacour, S., Verhoelst, T., Meimon, S., Mugnier, L., Thiébaut, E., Berger, J. P., Ridgway, S. T., Monnier, J. D., Millan-Gabet, R., and Traub, W., "Imaging the spotty surface of Betelgeuse in the H band," *A&A* **508**, 923–932 (2009).

[18] Lacour, S., Thiébaut, E., Perrin, G., Meimon, S., Haubois, X., Pedretti, E., Ridgway, S. T., Monnier, J. D., Berger, J. P., Schuller, P. A., Woodruff, H., Poncelet, A., Le Coroller, H., Millan-Gabet, R., Lacasse, M., and Traub, W., "The Pulsation of χ Cygni Imaged by Optical Interferometry: A Novel Technique to Derive Distance and Mass of Mira Stars," *ApJ* **707**, 632–643 (2009).